UCLA
UCLA Previously Published Works

Title

MEK Inhibition Sensitizes Pancreatic Cancer to STING Agonism by Tumor Cell-intrinsic Amplification of Type I IFN Signaling.

Permalink

https://escholarship.org/uc/item/8ck5926p

Journal

Clinical Cancer Research, 29(16)

Authors

Ghukasyan, Razmik
Liang, Keke
Chau, Kevin
et al.

Publication Date

2023-08-15

DOI

10.1158/1078-0432.CCR-22-3322

Peer reviewed

eScholarship.org Powered by the California Digital Library
University of California

Author Manuscript

Author Manuscript

Author Manuscript

Author Manuscript

HHS Public Access

Author manuscript

Clin Cancer Res. Author manuscript; available in PMC 2024 February 14.

Published in final edited form as:

Clin Cancer Res. 2023 August 15; 29(16): 3130–3141. doi:10.1158/1078-0432.CCR-22-3322.

MEK Inhibition Sensitizes Pancreatic Cancer to STING Agonism by Tumor Cell-intrinsic Amplification of Type I IFN Signaling

Razmik Ghukasyan[1,2], **Keke Liang**[1,3], **Kevin Chau**[4], **Luyi Li**[1], **Charlotte Chan**[1], **Evan R. Abt**[4,5], **Thuc Le**[4,5,6], **Joon Y. Park**[1], **Nanping Wu**[1], **Alykhan Premji**[1], **Robert Damoiseaux**[4,6], **Tony Luu**[4], **Amanda Labora**[1], **Khalid Rashid**[4,5], **Jason M. Link**[1,6], **Caius G. Radu**[2,4,5,6], **Timothy R. Donahue**[1,2,4,5,6]

[1]Department of Surgery, University of California Los Angeles, Los Angeles, California

[2]David Geffen School of Medicine, University of California Los Angeles, Los Angeles, California

[3]Department of General Surgery/Pancreatic and Thyroid Surgery, Shengjing Hospital of China Medical University, Shenyang, P.R. China

[4]Department of Molecular and Medical Pharmacology, University of California Los Angeles, Los Angeles, California

[5]Ahmanson Translational Imaging Division, UCLA, Los Angeles, California

[6]Jonsson Comprehensive Cancer Center, University of California Los Angeles, Los Angeles, California

Abstract

Purpose: Stimulator of interferon genes (STING) agonists are currently in development for treatment of solid tumors, including pancreatic ductal adenocarcinoma (PDAC). Response rates to STING agonists alone have been promising yet modest, and combination therapies will likely be required to elicit their full potency. We sought to identify combination therapies and mechanisms that augment the tumor cell–intrinsic effect of therapeutically relevant STING agonists apart from their known effects on tumor immunity.

Corresponding Authors: Timothy R. Donahue, University of California, Los Angeles, Suite 54-117 CHS, Los Angeles, CA 90095-6904. tdonahue@mednet.ucla.edu; and Caius G. Radu, cradu@mednet.ucla.edu.

R. Ghukasyan and K. Liang contributed equally to this article.

Authors' Contributions

R. Ghukasyan: Conceptualization, data curation, formal analysis, supervision, funding acquisition, validation, investigation, visualization, methodology, writing–original draft, project administration, writing–review and editing. **K. Liang:** Conceptualization, data curation, formal analysis, supervision, validation, visualization, methodology. **K. Chau:** Data curation, validation, methodology. **L. Li:** Conceptualization, data curation, formal analysis, validation, methodology. **C. Chan:** Conceptualization, data curation, formal analysis, validation, visualization, methodology. **E.R. Abt:** Conceptualization, data curation, formal analysis, supervision, validation, investigation, visualization, methodology, writing–review and editing. **T. Le:** Conceptualization, formal analysis, methodology. **J.Y. Park:** Data curation, validation, visualization, methodology. **N. Wu:** Data curation, methodology. **A. Premji:** Conceptualization, data curation, formal analysis, supervision, validation, visualization, methodology. **R. Damoiseaux:** Resources, validation, methodology. **T. Luu:** Methodology. **A. Labora:** Conceptualization, data curation, supervision, validation, methodology. **K. Rashid:** Conceptualization, data curation, formal analysis, validation, visualization, methodology. **J.M. Link:** Conceptualization, data curation, supervision, validation, visualization, methodology, writing–original draft, writing–review and editing. **C.G. Radu:** Conceptualization, resources, data curation, formal analysis, supervision, funding acquisition, validation, investigation, project administration, writing–review and editing. **T.R. Donahue:** Conceptualization, resources, data curation, supervision, funding acquisition, validation, investigation, writing–original draft, project administration, writing–review and editing.

Supplementary data for this article are available at Clinical Cancer Research Online (http://clincancerres.aacrjournals.org/).

Author Manuscript Author Manuscript Author Manuscript Author Manuscript

Experimental Design: We screened 430 kinase inhibitors to identify synergistic effectors of tumor cell death with diABZI, an intravenously administered and systemically available STING agonist. We deciphered the mechanisms of synergy with STING agonism that cause tumor cell death *in vitro* and tumor regression *in vivo*.

Results: We found that MEK inhibitors caused the greatest synergy with diABZI and that this effect was most pronounced in cells with high STING expression. MEK inhibition enhanced the ability of STING agonism to induce type I IFN-dependent cell death *in vitro* and tumor regression *in vivo*. We parsed NFκB-dependent and NFκB-independent mechanisms that mediate STING-driven type I IFN production and show that MEK signaling inhibits this effect by suppressing NFκB activation.

Conclusions: Our results highlight the cytotoxic effects of STING agonism on PDAC cells that are independent of tumor immunity and that these therapeutic benefits of STING agonism can be synergistically enhanced by MEK inhibition.

Introduction

Patients diagnosed with pancreatic ductal adenocarcinoma (PDAC) are faced with a 50% chance of death in under a year and a 12% chance of survival within 5 years (1). Although surgical resection of the primary tumor before metastatic spread is potentially curative, most patients progress to metastatic disease, which typically exhibits a response rate of only approximately 30% to standard-of-care chemotherapy (2, 3). Intertumoral heterogeneity and a typically immunosuppressive microenvironment remain substantial barriers to identifying effective treatments (4–6). Thus, precision medicine approaches that use drug-specific biomarkers to inform treatment along with immunomodulatory agents will likely be required to advance care for patients with PDAC. Recent progress using PARP inhibitors for patients with tumors that are defective in DNA damage repair (7) and immune checkpoint blockade (8, 9) have been promising but are effective for only a subset of patients with PDAC. Therapeutic agents that are broadly but specifically cytotoxic to tumor cells and that also promote tumor immunity will be promising therapeutic options.

Tumor immunity is strongly enhanced by activation of the stimulator of interferon genes (STING1, hereafter STING) pattern recognition receptor and consequent upregulation of type I IFN (10–12). STING is activated by intracellular cyclic dinucleotides from microbial pathogens or endogenous cytosolic cyclic 2′3′-GMP-AMP (cGAMP) synthesized by cyclic GMP-AMP synthase (cGAS) from cytosolic double-stranded DNA (13). Activated STING translocates from the endoplasmic reticulum to the Golgi apparatus where it recruits TANK-binding kinase 1 (TBK1) to phosphorylate IFN regulatory factor 3 (IRF3) and drive transcription of *IFNB1* (14, 15). In turn, secreted IFNB1 (IFN) acts via autocrine and paracrine signaling through IFN receptors and JAK/STAT signaling to upregulate transcription of hundreds of IFN-stimulated genes (ISG; ref. 16). Activation of STING in the tumor microenvironment (TME) triggers an innate immune response and inflammation that restricts tumor growth (17), an outcome that has been successfully leveraged clinically (18, 19). In parallel, STING signals through pathways independent of direct IRF3 activation —notably NFκB—to produce inflammatory cytokines (20). Moreover, STING expression

Author Manuscript Author Manuscript Author Manuscript Author Manuscript

itself is upregulated by positive feedback from IFN signaling (21) potentially augmenting the STING-mediated effects promoting tumor immunity.

Independent of the innate immune response, aberrant cell-cycle activity and replication stress in cancer cells yield cytosolic DNA and cGAS-derived cGAMP to activate STING and thus IFN signaling, resulting in intrinsic tumor cell cytotoxicity (22, 23). Most tumors escape this effect by inactivating STING and/or cGAS through genetic and epigenetic alterations (24, 25); however, STING is overexpressed in pancreatic tumors relative to adjacent nontumor tissue (26), increasing the potential for therapeutic efficacy of STING activators. STING can be indirectly activated by therapeutics that promote DNA damage and replication stress, but a new class of drugs has emerged that directly activate STING (27, 28). One of these—a novel, systemically delivered STING agonist (GSK3745417 or diABZI)—enhances tumor immunity in preclinical models and is now being tested in phase I clinical trials (NCT03843359, NCT05424380). While previous and ongoing studies of STING biology have mostly focused on the immunomodulatory properties of type I IFNs in the nonmalignant compartment of the TME (29–31), the goal of this study was to understand how STING agonists may additionally impact PDAC tumor biology through tumor cell-intrinsic cytotoxicity and to identify therapeutic codependencies that can be used to improve the treatment of PDAC.

In this study, we performed a high-throughput screen of 430 kinase inhibitors and identified MAP2K1 (MEK) inhibitors (MEKi) as the class of drugs with the greatest cytotoxic synergy with STING activation in PDAC cell lines. Using *in vitro* and *in vivo* PDAC models, we determined that the synergy is IFN dependent, and for maximal effect, required NFκB activity; however, it was independent of NFκB-driven proinflammatory cytokines. We demonstrate that STING-mediated activation of NFκB is essential for robust, IFN-mediated cytotoxicity, and we identify IRF1 as the mechanistic mediator between NFκB and IFN expression. In addition, we provide evidence that this role of NFκB is normally suppressed by MEK signaling. By relieving this suppression with MEK inhibition, the cytotoxic, tumor-restricting effect of STING agonism is dramatically augmented. Our results provide support for the use of combined STING agonism and MEK inhibition for the optimal therapeutic effects of immune-independent tumor cell cytotoxicity.

Materials and Methods

Cell culture

Panc03.27, HPAF-II, HS766T, CFPAC-1, SU.86.86, PANC-1, PANC10.05, KP3, PANC02.03, PANC02.13, ASPC1, PK59, BxPC-3, and SW 1990 were purchased from ATCC. DAN-G and YAPC were provided by Dr. David Dawson (University of California, Los Angeles, CA). AM1283 cultures were derived from a patient-derived xenograft (PDX) model provided by the NCI. SUIT2, T3M4, and PATU8988T were purchased from Research Resource Identifiers. PDXs, XWR200, and XWR7 were developed from UCLA patients who gave informed written consent and approved under Institutional Review Board Protocol No. 11-002112 in accordance with the U.S. Common Rule. KP4662 mouse tumor cells were a kind gift from Robert Vonderheide at the University of Pennsylvania (Philadelphia, PA). All cells were cultured in DMEM with 10% FBS and 1% penicillin/streptomycin at

Author Manuscript Author Manuscript Author Manuscript Author Manuscript

37°C in 5% CO_2. Cells were routinely authenticated by PCR and checked for *Mycoplasma* contamination with the PCR-based Venor *Mycoplasma* kit.

Drugs

Drug stocks were prepared in DMSO. All drugs and associated vendors are listed in the Key Resource Table (see Supplementary Data).

Animal studies

All animal studies were approved by UCLA Animal Research Committee. After trypsinization and washing with ice-cold PBS twice, 1×10^6 tumor cells suspended in 50-μL ice-cold PBS were inoculated subcutaneously in the flank(s) of 6- to 8-week-old female NOD-*Prkdc*^{em26Cd52}*Il2rg*^{em26Cd22}/NjuCrl-immunodeficient mice (NCG, Charles River). For XWR7, previously frozen tumor fragments were washed and suspended in ice-cold PBS prior to inoculation. Tumor volumes were determined by caliper measurements and estimated by applying the following formula: vol = $1/2xy^2$. All measurements and calculations were performed by trained technicians blinded to the experimental conditions. For doxycycline (DOX) treatment, mice were supplied with a control or DOX hyclate-supplemented diet intended to deliver 2 to 3 mg of DOX daily. For diABZI treatment, mice were administered 100 μL of 1.5 mg/kg diABZI or vehicle (40% PEG400 in 0.9% saline) by tail vein intravenous injection. Cobimetinib was administered by daily oral gavage of 50 μL in 5 mg/kg (5% DMSO in corn oil) doses.

Tumor homogenization

Thirty-mg fragments of resected tumors were harvested, snap-frozen in liquid nitrogen, and transferred to Omni Hard Tissue homogenization vials. A total of 750 μL of lysis buffer (50 mmol/L ammonium bicarbonate pH 7.2, 0.5% sodium deoxycholate, 12 mmol/L sodium laurel sarcosine) supplemented with protease and phosphatase inhibitor cocktails was added to each sample. Samples were homogenized with an Omni Bead Ruptor Elite (eight cycles of 15 seconds on, 30 seconds off, speed 8) with the device chilled to 4°C with liquid nitrogen. Tissue homogenates were cleared by centrifugation at 12,000 × *g* for 12 minutes at 4°C. Cleared lysates were normalized using the bicinchoninic acid (BCA) method and prepared for immunoblot analysis.

Immunoblot analysis

Cells were lysed in cold RIPA lysis buffer with protease and phosphatase inhibitors. The lysates were subsequently normalized using a BCA assay, then diluted using RIPA buffer and 6 × laemmli loading dye. Protein extracts were resolved on SDS-PAGE and then electrotransferred to an Immun-Blot Nitrocellulose membrane. After blocking in 5% nonfat milk or 5% BSA in TBS + 0.1% Tween-20 (TBS-T), membranes were incubated with the indicated primary antibodies (in 5% BSA, 0.02% sodium azide in TBS-T) at 4°C overnight. After incubation, the membranes were washed with TBS-T and then probed with horseradish peroxidase (HRP)-conjugated secondary antibodies (1:2,500 dilution in 5% BSA, TBS-T) at room temperature for 1 hour. Blots were developed using Immobilon Forte Western HRP Substrate and imaged on the LI-COR Oddessy imaging system. Primary

Author Manuscript Author Manuscript Author Manuscript Author Manuscript

antibodies were used at a 1:1,000 dilution and are reported in the Key Resource Table (see Supplementary Data).

qRT-PCR

Total RNA was extracted from cells using the NucleoSpin RNA kit. Reverse transcription was performed using the MultiScribe Reverse Transcriptase (Thermo Fisher Scientific). Quantitative PCR was performed using 2x qPCR Universal Green Master Mix (Lamda Biotech); reactions were run in the QuantStudio3 Applied Biosystems qRT-PCR machine. RNA expression values were normalized and calculated as relative expression to control. Primer sequences used for qRT-PCR for each gene are reported in the Key Resource Table (see Supplementary Data).

Human IFNβ ELISA assay

After 24 hours of incubation of CFPAC-1 cells with ± 1 μmol/L diABZI ± 100 nmol/L trametinib in biologic triplicates, 200 μL of cultured media was collected, and ELISA was performed to detect the levels of IFNβ by utilizing the VeriKline Human IFN Beta ELISA kit by PBL Assay Science.

Viability assay

For CellTiter-Glo analysis, cells were plated at 1×10^3 cells per 30 μL per well in white, opaque 384-well plates and treated as described. Following incubation, 50 μL of two-dimensional (2D) CellTiter-Glo reagent (diluted 1:5 in dPBS) was added to each well. The plates were incubated at room temperature for 5 minutes, and luminescence was measured using a BioTek microplate luminescence reader.

Annexin V flow cytometric apoptosis assay

After incubating CFPAC-1 cells in ± 1 μmol/L diABZI ± 100 nmol/L trametinib in triplicates for 72 hours, cells were collected, washed twice with ice-cold PBS, and stained with Annexin V-FITC and propidium iodide (PI) by utilizing the reagents and protocols outlined in the Annexin-V-FITC Apoptosis Kit. Untreated CFPAC-1 cells were incubated for 20 minutes at 55°C and used as positive controls for apoptosis. Unstained, Annexin V-FITC or PI-stained controls were used to properly set the flow cytometer. Attune NxT Flow Cytometer at UCLA Jonsson Comprehensive Cancer Center Flow Cytometry Core was used for data collection. Flowjo v10 software was used for data analyses.

CRISPR-Cas9 and guide RNA-guided gene knockout

Three guide RNAs (gRNA) for each targeted gene (*STING, IFNAR1, IL6R*, and *IRF1*—see Key Resource Table (see Supplementary Data) for gRNA sequences) were designed and purchased from IDT. For each reaction, 1×10^5 CFPAC1 or SUIT2 cells were electroporated under optimized condition with the NEON system. Specifically, 5-μg recombinant s.p.Cas9 (No. 1081058, IDT) and 50-pmol gRNA were combined at room temperature for 15 minutes, then mixed with 10-μL cells. After electroporation, cells were cultured in a 12-well plate overnight, and DNA was extracted for genomic PCR and Tracking of Indels by Decomposition (TIDE) analysis (http://tide.nki.nl) to assess knockout (KO) efficiency. Two

Author Manuscript Author Manuscript Author Manuscript Author Manuscript

gRNAs with the best knockout effect were selected. Single-cell cloning was performed with limited dilution of cells into 96-well plates. At least two single clones of each gRNA were confirmed with immunoblot analysis and TIDE analysis.

CFPAC-1 TetR STING^{R284M} design and generation

The generation of CFPAC-1 TetR-STING^{R284M} cells was described previously (32). A STING^{R248M} encoding gene fragment was ligated into the pENTR-D/TOPO entry vector. Resulting constructs were recombined into pLenti-CMV/TO-GFP/PURO using Gateway LR Clonase II. For virus production, lentivirval vectors and packaging plasmids (psPAX2, pMD2G) at a 2:1:1 ratio were transfected into FT293 cells using polyethylenimine. Cells were selected in puromycin for 1 week. Gene expression was regulated by the DOX responsive Tet repressor (TetR) protein expressed from the pLenti3/EF/GW/IVS-Kozak-TetR-P2A-Bsd vector.

Small-molecule kinome screen

A library of 430 protein kinase inhibitors (SelleckChem, catalog No. L1200) was arrayed in polypropylene 384-well plates at 200 × concentrations covering a 7-point concentration range (corresponding to 1× concentrations: 5 μmol/L, 1.65 μmol/L, 550 nmol/L, 185 nmol/L, 61.5 nmol/L, 20.6 nmol/L, 6.85 nmol/L). A total of 25 μL per well of growth media with or without 2 μmol/L diABZI supplementation (for a final concentration of 1 μmol/L) was plated in opaque-white 384-well plates using a BioTek multidrop liquid handler. Protein kinase inhibitors were added by 250-nL pin-tool transfer (BioMek FX, Beckman-Coulter), and inhibitor/media mixtures were incubated at room temperature for 30 minutes. A total of 25 μL of a 40,000 cells/mL CFPAC-1 suspension (for 1,000 cells/well) was subsequently added to each well. After 72 hours, 50 μL of 2D CellTiter-Glo reagent diluted 1:5 in PBS was added to each well, and luminescence readings were performed using a Wallac plate reader (Perkin Elmer). Each condition was assayed in duplicate, and percent proliferation values were calculated by normalizing experimental wells to plate negative controls and averaging replicate values. Composite diABZI synergy scores for each test compound were defined as the sum of the Bliss additivity score (percentage proliferation inhibition observed – percentage proliferation inhibition expected) between diABZI and individual protein kinase inhibitor concentrations across the 7-point concentration range. Z factor scores for individual assay plates were calculated using eight positive and eight negative control wells on each plate as described previously (33). All plates gave a Z factor > 0.5.

RNA sequencing

CFPAC-1 PDAC cells were plated in 6-well plates and treated ± 1 μmol/L diABZI ± 100 nmol/L trametinib for 24 hours. Following treatment, mRNA was extracted as described for RT-PCR analysis and processed for next-generation sequencing. The analysis workflow consisted of mRNA capture, cDNA generation, end repair to generate blunt ends, A-tailing, adaptor ligation, and PCR amplification. Libraries were sequenced on Illumina HiSeq 3000 on a single-read 50-bp run. An FDR of <0.01% was applied to filter significantly altered transcripts. Heatmaps were generated by utilizing the Phantasus platform available through

Author Manuscript Author Manuscript Author Manuscript Author Manuscript

https://artyomovlab.wustl.edu/phantasus. The list of genes with statistically significant alterations were submitted to ENRICHR MSigDB Hallmark pathway analysis platform.

Luminex

CFPAC-1 PDAC cells were plated in 6-well plates and treated ± 1 μmol/L diABZI ± 100 nmol/L trametinib for 24 hours. Following treatment, 200 μL of cultured media was collected in three biologic replicates and submitted to UCLA Department of Pathology and Laboratory Medicine Immune Assessment Core. Luminex's xMAP immunoassay platform was utilized to run a human cytokine/chemokine 38-plex panel.

Statistical analyses

Data are presented as mean ± SEM with the indicated number of biological replicates. Comparisons of two groups were calculated using unpaired two-tailed Student *t* test, and *P* values less than 0.05 were considered significant. Comparisons of more than two groups were calculated using one-way ANOVA followed by Bonferroni multiple comparison tests, and *P* values less than 0.05/*m*, where *m* is the total number of possible comparisons, were considered significant. All analyses were conducted by using Prism Version 8.4.2.

Data availability

All data are available on request from the corresponding author.

Results

Pharmacologic STING activation and MAPK pathway inhibition are synergistically cytotoxic in PDAC cell lines with high STING expression

A hallmark function of STING activation is upregulation of *IFNB1* transcription. We assessed *IFNB1* expression in a panel of PDAC cell lines in response to the STING agonist, diABZI and found that it enhanced *IFNB1* expression in all cell lines, with the greatest increase in CFPAC-1 cells (Fig. 1A). We used CFPAC-1 cells to identify potential synergy between diABZI and any of 430 kinase inhibitors. From this high-throughput screen, we identified seven MEKi among the top 10 compounds with the greatest synergy (Fig. 1B). In contrast, JAK inhibitors antagonized the effects of STING activation, consistent with JAK/STAT signaling as an essential mediator of IFN cytotoxicity (Fig. 1B). As expected, MAPK pathway inhibition by ERK inhibitors also functioned synergistically with diABZI in CFPAC-1 cells, though less effectively than MEKi (Fig. 1B). STING was essential for the effect of diABZI and the MEKi, trametinib, as synergy was lost in CFPAC-1 cells after CRISPR/Cas9-mediated knockout of *STING* (Supplementary Fig. S1A and S1C) or upon inhibition of the essential STING cofactor, TBK1 (Fig. 1C). We also found synergy between MEK inhibition and STING agonism in several other human PDAC cell lines demonstrating that this effect is not specific to CFPAC-1 cells (Supplementary Fig. S1B). Among these cell lines, STING expression (Fig. 1D) clearly correlated with high synergy (Fig. 1E), suggesting that baseline STING expression can predict responses to the combined effect of STING activation and MEK inhibition. To determine whether the inhibitory effect of MEK inhibition and STING agonism is cytotoxic, we measured cell death by flow cytometry and found that the synergy caused significantly more cell death (Fig. 1F). To

Author Manuscript Author Manuscript Author Manuscript Author Manuscript

test whether apoptosis was a component of cell death, we performed the drug response assay in the presence of ZVAD-FMK (InvivoGen) and identified a 44% reduction in the percentage of early apoptotic cells (Annexin V+ PI^{neg}) but a much smaller change in the percentage of Annexin V+ PI+ cells (Supplementary Fig. S1C) suggesting that apoptosis plays a role but may not be solely responsible for the cell death induced by diABZI and trametinib. Accordingly, we found an increase in cleaved PARP, caspase 3, and caspase 9 after treatment with both diABZI and trametinib (Fig. 1G). Mechanistically, we identified a trametinib-dependent increase in BIM_{EL} expression that was augmented by the addition of diABZI (Supplementary Fig. S1D), highlighting a potential mechanism for the apoptotic component of cell death.

STING signaling and MEK inhibition synergistically suppress tumor growth *in vivo*

To test the acute effects of STING activation *in vivo*, we designed a CFPAC-1 cell line with a DOX-inducible expression of constitutively active STING (CFPAC-1 TetR $STING^{R284M}$; ref. 34) and resultant phosphoactivation of IRF3, IFN-driven activation of STAT1, and expression of the ISG; STAT1 and MX1 (Fig. 2A). As expected, trametinib had no effect on DOX-induced $STING^{R284M}$ protein expression in CFPAC-1 TetR $STING^{R284M}$ cells (Supplementary Fig. S2A), similar to the limited effect of trametinib on diABZI-activated STING in the parental CFPAC-1 cell line (Supplementary Fig. S2A). *In vivo*, the combined effect of DOX and the MEKi, cobimetinib synergistically suppressed subcutaneous xenografts of CFPAC-1 TetR $STING^{R284M}$ cells (Fig. 2B; Supplementary Fig. S2B); likewise, xenografts of the parental CFPAC-1 cell line were synergistically suppressed by diABZI and cobimetinib (Fig. 2C; Supplementary Fig. S2C). Similarly, the combination of diABZI and cobimetinib synergistically suppressed tumor growth in mice with subcutaneous xenografts of a patient-derived tumor (XWR7; Fig. 2D; Supplementary Fig. S2D and S2E). Consistent with STING and IFN driving these *in vivo* effects, 24-hour treatment with diABZI phosphoactivated IRF3 leading to IFN-driven STAT1 phosphorylation and expression of the ISG; IFIT1 and TYMP in XWR7 tumors (Supplementary Fig. S2F).

We found similar efficacy of the diABZI+cobimetinib combination in an *in vivo* syngeneic mouse tumor model using a cell line (KP4662) from the genetically engineered KPC PDAC model implanted to C57BL/6 hosts (Supplementary Fig. S2G and S2H). Moreover, we observed enhanced efficacy of diABZI in this model—relative to tumors in immunodeficient hosts—that appeared later than effects of the drug combination (Supplementary Fig. S2G and S2H). At endpoint, we observed more $CD8^+$ T-cell infiltrates, more inflammatory M1 macrophages, and fewer suppressor M2 macrophages in tumors from mice treated with diABZI with or without cobimetinib (Supplementary Fig. S2I). These data are consistent with immunostimulatory effects of diABZI superimposed on the cytotoxic tumor cell–intrinsic effect of the drug combination.

MEK inhibition amplifies STING-driven IFN and NFκB activity *in vitro* and *in vivo*

Cytotoxicity mediated by type I IFN signaling is tumor suppressive. On the basis of our results, we hypothesized that STING-mediated production of type I IFN and/or its downstream effector cytokines are augmented by MEK inhibition. To address this concept, we assessed gene expression by RNA sequencing (RNA-seq) of CFPAC-1 cells exposed

Author Manuscript Author Manuscript Author Manuscript Author Manuscript

to diABZI with or without trametinib for 24 hours and identified 586 genes upregulated by diABZI that were further upregulated by the combination of diABZI and MEK inhibition (Fig. 3A, left). We assessed the ontology of this gene set with ENRICHR and identified significant associations with a type I IFN response, TNFα and IL6 signaling, and inflammation (Fig. 3A, right). We confirmed RNA-seq gene expression by RT-PCR and found that *IFNB1* transcription was significantly higher when CFPAC-1 cells were exposed to the combination of diABZI and trametinib compared with diABZI alone (Fig. 3B). We found the same significant effect in four additional human PDAC cell lines (Supplementary Fig. S3A), though to a lesser degree than CFPAC-1 cells. *IFNB1* transcription in CFPAC-1 cells was also upregulated by a cGAS substrate (interferon stimulatory DNA; Supplementary Fig. S3B), cGAMP activation of STING (Supplementary Fig. S3C), and when STING agonism was combined with cobimetinib (Supplementary Fig. S3D). As expected, secreted IFNβ was detected in the supernatant of CFPAC-1 cell cultures (Fig. 3C). We also observed downstream effects of IFN signaling—namely, phosphoactivation of STAT1 and STAT3, and increased protein expression of transcriptional targets of IFNβ signaling, MX1 and IFIT1 (Fig. 3D, left); SUIT2 cells were similarly affected (Fig. 3D, right). We confirmed that the combination of STING agonism and MEK inhibition triggers IFN signaling *in vivo* by identifying phosphoactivation of STAT1 and increased expression of MX1 and IFIT1 in CFPAC-1 xenografts treated *in vivo* with diABZI and cobimetinib for 24 hours (Fig. 3E).

In line with enrichment of the NFκB pathway (Fig. 3A), the combination of diABZI and trametinib increased transcription of *IL6* and *TNF* in both CFPAC-1 (Fig. 3F) and SUIT2 cells (Supplementary Fig. S3E). Extracellular IL6, TNF, IL1A, and IFNβ levels were elevated in diABZI-treated CFPAC-1 cells compared to diABZI alone, indicating increased activation of NFκB (Fig. 3G; Supplementary Table S1).

Type I IFN signaling is essential for the synergy between STING activation and MEK inhibition *in vitro* and *in vivo*

The combination of STING activation and MEK inhibition drove signaling and cytokine production that is related to both IFNβ and NFκB. Thus, we investigated whether IFNβ signaling alone was necessary and/or sufficient for the cytotoxic effects of the drug combination. To accomplish this, we generated both CFPAC-1 and SUIT2 cells with CRISPR/Cas9-mediated deletion of the IFNα receptor 1 (IFNAR1)-KO and demonstrated that these cells could not upregulate ISG in response to exogenous IFN (Supplementary Fig. S4A). IFNAR1-KO cells were unable to phosphoactivate STAT1 in response to diABZI and trametinib (Supplementary Fig. S4B), and as an expected consequence, were unaffected in cell culture by the addition of diABZI to trametinib (Fig. 4A). These results were validated *in vivo*, as the addition of diABZI to cobimetinib treatment had an insignificant impact on survival (Fig. 4B) and tumor growth (Fig. 4C) in mice with IFNAR-KO xenografts despite synergy between diABZI and cobimetinib in mice with xenografts of the parental CFPAC-1 cell line. Consistent with our previous *in vitro* results (Fig. 1F and G), parental CFPAC-1 xenografts expressed markers of apoptosis 24 hours after a single dose of diABZI that was further elevated by treatment with the diABZI and cobimetinib combination (Fig. 4D). In contrast, there was no evidence of apoptosis in IFNAR1-KO CFPAC-1 xenografts (Fig. 4D). These results demonstrated that IFNβ signaling is necessary for the cytotoxic effect

Author Manuscript Author Manuscript Author Manuscript Author Manuscript

of diABZI and MEK inhibition. Mechanistically, exogenous IFN phenocopied the effects of STING activation (Supplementary Fig. S4C), but deletion of IFNAR was insufficient to ablate expression of some diABZI-influenced ISG (MX1 and IFIT1; Supplementary Fig. S4B and S4C). These data indicate that STING-driven, IFN-mediated cytotoxicity may depend on a unique pattern of ISG distinct from that induced by IFN alone, consistent with previous reports of IFN-independent ISG expression (35, 36).

NFκB-driven expression of IRF1 but not IL6 contributes to the synergistic effects of STING activation and MEK inhibition

STING activation promotes both a cytotoxic IFN response and a proinflammatory response directed by NFκB. We confirmed that STING agonism promoted phosphoactivation of TBK1 and IRF3 concomitantly with activation of NFκB in CFPAC-1 cells (Fig. 5A). As expected, MEK inhibition did not influence phosphorylation of TBK1 or IRF3, but it did augment STING-driven activation of NFκB (Fig. 5A), suggesting that NFκB may mediate the synergistic effects of STING agonism and MEK inhibition. Consistent with this, we found that inhibition of IKKβ (the required mediator of NFκB activation) with TPCA1 significantly reduced *IFNB1* transcription induced by diABZI with and without trametinib (Fig. 5B) and similarly reduced expression of NFκB-regulated cytokines, *IL6* and *TNF* (Fig. 5C).

NFκB-driven expression of IL6 and signaling through its receptor (IL6R) can promote inflammation, apoptosis, and senescence. Thus, we considered that IL6 signaling may be necessary for—or contribute to—apoptosis mediated by IFN upon STING agonism. However, we found no change in the response to diABZI and trametinib when IL6R was inhibited with tocilizumab (Supplementary Fig. S5A and S5B) nor when IL6R was genetically ablated in SUIT2 cells (Supplementary Fig. S5C). Moreover, the absence of IL6R in SUIT2 cells prevented recombinant IL6 from activating its downstream effector, STAT3, but did not prevent phosphoactivation of STAT3 by diABZI and trametinib (Supplementary Fig. S5D). These data underscore the dominant role played by IFN in tumor cell suppression mediated by STING agonism and MEK inhibition.

IRFs are well-known transcriptional targets of NFkB. We assessed expression of *IRF* genes in our RNA-seq dataset and found that diABZI and trametinib caused a synergistic increase in several IRF family members after stimulation (Fig. 5D). Among these, *IRF1* is an exceptionally strong regulator of *IFNB1* chromatin accessibility and is strongly induced by NFkB (37, 38). We used TPCA-1 to confirm *IRF1* as a target of NFkB in CFPAC-1 cells (Fig. 5E) and demonstrated that the robust increase in *IRF1* induced by diABZI and trametinib was NFkB dependent (Fig. 5E). In addition, genetic ablation of *IRF1* in CFPAC-1 cells slightly diminished the effects of diABZI—but nearly ablated the synergistic effects of diABZI and trametinib—on *IFNB1* expression (Fig. 5F).

STING-driven cytotoxicity is inhibited by concomitant activation of MEK and subsequent negative regulation of NFκB

Our results indicate that IRF1 expression downstream of NFκB activation contributes to the IFN-mediated cytotoxicity driven by STING agonism, but that STING cannot

Author Manuscript Author Manuscript Author Manuscript Author Manuscript

fully activate NFκB in the presence of MEK activity. NFκB activity can be negatively regulated by MEK signaling. As a consequence of IKKβ phosphorylating NFκB, tumor progression locus 2 (TPL2) is made available to activate its substrate, MEK (39). We pharmacologically inhibited TPL2 and as expected, observed a decrease in diABZI-dependent ERK phosphorylation after only 3 hours (Fig. 6A) and an increase in NFκB phosphorylation after 24 hours (Fig. 6A). By comparison, trametinib was more effective at suppressing ERK activation and relieving MEK-mediated inhibition of NFκB than TPL2 inhibition (Fig. 6A), suggesting that TPL2 is only partially responsible for MEK activation in the context of STING activation. In line with these results, STING-driven expression of IRF1 (Fig. 6B) and transcription of *IFNB1, IL6*, and *TNFA* (Fig. 6C) were significantly increased by inhibiting TPL2, although not as effectively as with trametinib.

Discussion

In this study, we describe a mechanism for intrinsic STING-driven cytotoxicity in PDAC tumors that underlies an insufficiently explored benefit of STING-agonist therapy. We show that this is especially relevant to PDAC tumors that—unlike most tumors—express high amounts of STING. Because single-agent therapies have shown marginal clinical benefit in PDAC, we screened for drugs that could act synergistically with a STING agonist and identified MEKi among the most effective. STING agonism and MEK inhibition in combination promoted apoptosis of PDAC tumor cells both *in vitro* and *in vivo* that seemed to be dependent on tumor cell STING expression levels. MEK inhibition strongly augmented the ability of STING to drive both IFN and NFκB production, and the cytotoxic effects of the synergy were dependent on signaling through the IFNα receptor. Although the NFκB transcriptional target, proinflammatory IL6 was dispensable for cytotoxicity, NFκB activation itself was required for the synergy. Mechanistically, we demonstrated that MEK inhibition derepressed NFκB activation, leading to more IRF1 expression, priming of IRF3 targets for transcription, and a resultant increase in IFN production; it is also likely that NFκB directly promotes transcription of *IFNB1* (40). As an ISG, STING expression is an expected consequence of IFN signaling; thus, completing a feed-forward cycle that may augment the cytotoxic effects of diABZI and MEK inhibition (Fig. 7). Our work identifies the participants and requirements for maximizing the therapeutic potential of STING agonists to drive tumor cell–intrinsic cytotoxicity, apart from its effects on tumor immunity.

Within the PDAC tumor environment, STING is expressed in leukocytes (29), cancer-associated fibroblasts (41), and endothelial cells (42), and its activation can lead to dramatic alterations in tumor immunity (31, 43). These radical, immunostimulatory changes in the PDAC TME certainly contribute to the efficacy of STING agonists, yet the complexity and robustness of STING activation within the TME has eclipsed the critical role for STING activation and autocrine cytotoxicity in tumor cells themselves. Moreover, the variation in STING expression and correlative responses to STING agonists among PDAC cell lines suggest that a biomarker-guided approach may help select patients and maximize the benefits of STING-driven autocrine cytotoxicity, especially in combination with broader effects in the TME. Our data also reveal that MEK inhibition may further augment the effects of STING agonists and may be specifically relevant to tumor cell–intrinsic

Author Manuscript Author Manuscript Author Manuscript Author Manuscript

cytotoxicity. Other intracellular, nucleic acid–sensing receptors like RIG-I (44) and TLR7 (37, 38) may similarly synergize with MAP kinase pathway inhibition and IRF1-mediated activation of IFN and ISG.

More than 90% of PDAC tumors are driven by activating mutations in *KRAS*, and many of the remainder harbor other mutations that activate RAF (45), promoting mitogenic and survival signaling through the MAPK pathway. Therapeutic inhibition of the MAPK pathway alone has modest efficacy and is characterized by cytostasis of tumor cells rather than cytotoxicity—adaptive resistance is common (46). This may underly the failure of trametinib to improve outcomes with gemcitabine in PDAC (47). In our study, we demonstrated that MEK can suppress NFκB (and consequently, reduce IFN expression), but that MEK inhibition alone is insufficient to drive NFκB and IFN-mediated cytotoxicity —this effect required synergy with STING activation. The role of NFκB in the synergistic cytotoxicity is primarily through its ability to enhance IFN expression, rather than through production of inflammatory cytokines like IL6. Thus, NFκB may be a key mediator of the duality of the STING effect by promoting tumor cell cytotoxicity through IFN while concomitantly promoting inflammatory tumor immunity in the TME.

Exogenous IFN alone can phenocopy the effects of STING activation but leads to toxicities and variable efficacy as a cancer therapeutic, despite several decades of trials. One concern with exogenous IFN as a therapeutic is that tumors may have been regularly exposed to endogenous IFN, shaping cancer cell evolution toward resistance. In fact, cancers commonly develop resistance to radiotherapy (48), chemotherapy (49), and immunotherapy (50)—as well as to IFN itself—by deleting IFN genes and disrupting IFN signaling (51, 52). This may explain the insensitivity of some PDAC cell lines to diABZI in our study, even when combined with MEK inhibition (Supplementary Fig. S1B). Chronic IFN production in tumors also leads to a state of tolerance termed IFN-related DNA damage resistance (49, 53); tumors with this phenotype enigmatically express chronic, low levels of IFN along with many ISG, yet exhibit none of the consequences expected from acute IFN exposure. This may reflect many cell types in the TME adopting mechanisms that normally limit the IFN response during chronic viral infections. However, our data suggest that PDAC tumor cells may still be intrinsically sensitive to STING-driven IFN—especially in the context of MEK inhibition—despite an IFN-tolerant TME.

We report that the cytotoxic effects of STING activation are normally constrained by MEK signaling in PDAC tumor cells, but that MEK inhibition leads to a synergistic boost in IFN-mediated cytotoxicity. We previously demonstrated that inhibition of ATR during IFN signaling leads to nucleotide insufficiency and replication stress–related cytotoxicity in PDAC, and as an extension, that STING-driven tumor cell cytotoxicity is also enhanced by ATR inhibition (54). Thus, MEK inhibition would predictably further sensitize tumor cells to replication stress in the context of ATR inhibition. Targeting both MEK and ATR may strongly enhance the underappreciated role for STING agonists in driving autocrine tumor cell cytotoxicity, and their effects would predictably compound the tumor cell–extrinsic effects of STING activation in the TME. Small-molecule inhibition of KRAS is another therapeutic approach that is an increasingly realistic treatment for PDAC. We have identified that the STING pathway and STING agonism activates the MAPK pathway through TPL2,

Author Manuscript Author Manuscript Author Manuscript Author Manuscript

which is a direct activator of MEK and downstream of KRAS. Therefore, in PDAC where STING is highly expressed in tumor cells (26), STING activation may be a source of persistent MAPK activity and resistance to emerging allelic specific inhibitors of mutant KRAS (55). This may be particularly pertinent if KRAS inhibitors are combined with STING agonists in pancreatic cancer.

Supplementary Material

Refer to Web version on PubMed Central for supplementary material.

Acknowledgments

T.R. Donahue and C.G. Radu are supported by R01CA250529. R. Ghukasyan received support from T32DK007180. This work was supported by the Hirshberg Foundation.

Authors' Disclosures

N. Wu reports grants from the NIH during the conduct of the study. R. Damoiseaux is a consultant for Amgen, Panorama Medicine, Forcyte Biotechnologies, and Pharma15. R. Damoiseaux is also co-founder of Pharma15, Forcyte Biotechnologies, and Enspire Bio. C.G. Radu reports grants from Revolution Medicines and other support from Sofie Biosciences and Trethera Corporation outside the submitted work. T.R. Donahue reports grants from NCI/NIH during the conduct of the study and personal fees and other support from Trethera Corporation outside the submitted work. No disclosures were reported by the other authors.

References

1. Siegel RL, Miller KD, Wagle NS, Jemal A. Cancer statistics, 2023. CA Cancer J Clin 2023;73:17–48. [PubMed: 36633525]
2. Conroy T, Desseigne F, Ychou M, Bouché O, Guimbaud R, Bécouarn Y, et al. FOLFIRINOX versus gemcitabine for metastatic pancreatic cancer. N Engl J Med 2011;364:1817–25. [PubMed: 21561347]
3. Von Hoff DD, Ervin T, Arena FP, Chiorean EG, Infante J, Moore M, et al. Increased survival in pancreatic cancer with nab-paclitaxel plus gemcitabine. N Engl J Med 2013;369:1691–703. [PubMed: 24131140]
4. Liudahl SM, Betts CB, Sivagnanam S, Morales-Oyarvide V, da Silva A, Yuan C, et al. Leukocyte heterogeneity in pancreatic ductal adenocarcinoma: phenotypic and spatial features associated with clinical outcome. Cancer Discov 2021;11:2014–31. [PubMed: 33727309]
5. Helms E, Onate MK, Sherman MH. Fibroblast heterogeneity in the pancreatic tumor microenvironment. Cancer Discov 2020;10:648–56. [PubMed: 32014869]
6. Steele NG, Carpenter ES, Kemp SB, Sirihorachai VR, The S, Delrosario L, et al. Multimodal mapping of the tumor and peripheral blood immune landscape in human pancreatic cancer. Nat Cancer 2020;1:1097–112. [PubMed: 34296197]
7. Golan T, Hammel P, Reni M, Van Cutsem E, Macarulla T, Hall MJ, et al. Maintenance olaparib for germline BRCA-mutated metastatic pancreatic cancer. N Engl J Med 2019;381:317–27. [PubMed: 31157963]
8. Casolino R, Corbo V, Beer P, Hwang C-I, Paiella S, Silvestri V, et al. Germline aberrations in pancreatic cancer: implications for clinical care. Cancers 2022;14:3239. [PubMed: 35805011]
9. Bockorny B, Grossman JE, Hidalgo M. Facts and hopes in immunotherapy of pancreatic cancer. Clin Cancer Res 2022;28:4606–17. [PubMed: 35775964]
10. Barber GN. STING: infection, inflammation and cancer. Nat Rev Immunol 2015;15:760–70. [PubMed: 26603901]
11. Ishikawa H, Ma Z, Barber GN. STING regulates intracellular DNA-mediated, type I interferon-dependent innate immunity. Nature 2009;461:788–92. [PubMed: 19776740]

Author Manuscript Author Manuscript Author Manuscript Author Manuscript

12. Vanpouille-Box C, Demaria S, Formenti SC, Galluzzi L. Cytosolic DNA sensing in organismal tumor control. Cancer Cell 2018;34:361–78. [PubMed: 30216189]
13. Ritchie C, Carozza JA, Li L. Biochemistry, cell biology, and pathophysiology of the innate immune cGAS-cGAMP-STING pathway. Annu Rev Biochem 2022;91:599–628. [PubMed: 35287475]
14. Kwon J, Bakhoum SF. The cytosolic DNA-sensing cGAS-STING pathway in cancer. Cancer Discov 2020;10:26–39. [PubMed: 31852718]
15. Yum S, Li M, Frankel AE, Chen ZJ. Roles of the cGAS-STING pathway in cancer immunosurveillance and immunotherapy. Annu Rev Cancer Biol 2019;3:323–44.
16. Rusinova I, Forster S, Yu S, Kannan A, Masse M, Cumming H, et al. INTERFEROME v2.0: an updated database of annotated interferon-regulated genes. Nucleic Acids Res 2013;41:D1040–6. [PubMed: 23203888]
17. Gan Y, Li X, Han S, Liang Q, Ma X, Rong P, et al. The cGAS/STING pathway: a novel target for cancer therapy. Front Immunol 2022;12:795401. [PubMed: 35046953]
18. Ramanjulu JM, Pesiridis GS, Yang J, Concha N, Singhaus R, Zhang S-Y, et al. Design of amidobenzimidazole STING receptor agonists with systemic activity. Nature 2018;564:439–43. [PubMed: 30405246]
19. Le Naour J, Zitvogel L, Galluzzi L, Vacchelli E, Kroemer G. Trial watch: STING agonists in cancer therapy. Oncoimmunology 2020;9:1777624. [PubMed: 32934881]
20. Wu J, Yan N. No longer a one-trick pony: STING signaling activity beyond interferon. J Mol Biol 2022;434:167257. [PubMed: 34627792]
21. Ma F, Li B, Yu Y, Iyer SS, Sun M, Cheng G. Positive feedback regulation of type I interferon by the interferon-stimulated gene STING. EMBO Rep 2015;16:202–12. [PubMed: 25572843]
22. Hayman TJ, Baro M, MacNeil T, Phoomak C, Aung TN, Cui W, et al. STING enhances cell death through regulation of reactive oxygen species and DNA damage. Nat Commun 2021;12:2327. [PubMed: 33875663]
23. Parker BS, Rautela JHertzog PJ. Antitumour actions of interferons: implications for cancer therapy. Nat Rev Cancer 2016;16:131–44. [PubMed: 26911188]
24. Konno H, Yamauchi S, Berglund A, Putney RM, Mulé JJ, Barber GN. Suppression of STING signaling through epigenetic silencing and missense mutation impedes DNA damage mediated cytokine production. Oncogene 2018;37:2037–51. [PubMed: 29367762]
25. Falahat R, Berglund A, Putney RM, Perez-Villarroel P, Aoyama S, Pilon-Thomas S, et al. Epigenetic reprogramming of tumor cell–intrinsic STING function sculpts antigenicity and T cell recognition of melanoma. Proc Natl Acad Sci U S A 2021;118:e2013598118. [PubMed: 33827917]
26. Liu F, Jiang M, Mei Z, Lin C, Tian L. cGAS-STING signalings potentiate tumor progression via sustaining cancer stemness. Transl Oncol 2022;20:101404. [PubMed: 35364558]
27. Holmes B. The potential of STING agonists is explored in cancer. Target Ther Oncol 2022;11:63.
28. Ding C, Song Z, Shen A, Chen T, Zhang A. Small molecules targeting the innate immune cGAS-STING-TBK1 signaling pathway. Acta Pharm Sin B 2020;10:2272–98. [PubMed: 33354501]
29. Woo S-R, Fuertes MB, Corrales L, Spranger S, Furdyna MJ, Leung MYK, et al. STING-dependent cytosolic DNA sensing mediates innate immune recognition of immunogenic tumors. Immunity 2014;41:830–42. [PubMed: 25517615]
30. Kabashima A, Matsuo Y, Ito S, Akiyama Y, Ishii T, Shimada S, et al. cGAS-STING signaling encourages immune cell overcoming of fibroblast barricades in pancreatic cancer. Sci Rep 2022;12:10466. [PubMed: 35773436]
31. Chamma H, Vila IK, Taffoni C, Turtoi A, Laguette N. Activation of STING in the pancreatic tumor microenvironment: a novel therapeutic opportunity. Cancer Lett 2022;538:215694. [PubMed: 35489447]
32. Moore AM, Zhou L, Cui J, Li L, Wu N, Yu A, et al. NAD+ depletion by type I interferon signaling sensitizes pancreatic cancer cells to NAMPT inhibition. Proc Natl Acad Sci U S A 2021;118:e2012469118. [PubMed: 33597293]
33. Zhang JH, Chung TDY, Oldenburg KR. A simple statistical parameter for use in evaluation and validation of high throughput screening assays. J Biomol Screen 1999;4:67–73. [PubMed: 10838414]

Author Manuscript Author Manuscript Author Manuscript Author Manuscript

34. Tang ED, Wang CY. Single amino acid change in STING leads to constitutive active signaling. PLoS One 2015;10:e0120090. [PubMed: 25790474]
35. Hasan M, Koch J, Rakheja D, Pattnaik AK, Brugarolas J, Dozmorov I, et al. Trex1 regulates lysosomal biogenesis and interferon-independent activation of antiviral genes. Nat Immunol 2013;14:61–71. [PubMed: 23160154]
36. Ashley CL, Abendroth A, McSharry BP, Slobedman B. Interferon-independent innate responses to cytomegalovirus. Front Immunol 2019;10:2751. [PubMed: 31921100]
37. Song R, Gao Y, Dozmorov I, Malladi V, Saha I, McDaniel MM, et al. IRF1 governs the differential interferon-stimulated gene responses in human monocytes and macrophages by regulating chromatin accessibility. Cell Rep 2021;34:108891. [PubMed: 33761354]
38. Yang L, Ding JL. MEK1/2 inhibitors unlock the constrained interferon response in macrophages through IRF1 signaling. Front Immunol 2019;10:2020. [PubMed: 31507609]
39. Gantke T, Sriskantharajah S, Ley SC. Regulation and function of TPL-2, an IκB kinase-regulated MAP kinase kinase kinase. Cell Res 2011;21:131–45. [PubMed: 21135874]
40. Panne D, Maniatis T, Harrison SC. An atomic model of the interferon-β enhanceosome. Cell 2007;129:1111–23. [PubMed: 17574024]
41. Baird JR, Friedman D, Cottam B, Dubensky TW, Kanne DB, Bambina S, et al. Radiation therapy combined with novel STING-targeting oligonucleotides results in regression of established tumors. Cancer Res 2016;76:50–61. [PubMed: 26567136]
42. Demaria O, De Gassart A, Coso S, Gestermann N, Di Domizio J, Flatz L, et al. STING activation of tumor endothelial cells initiates spontaneous and therapeutic antitumor immunity. Proc Natl Acad Sci U S A 2015;112:15408–13. [PubMed: 26607445]
43. Jing W, McAllister D, Vonderhaar EP, Palen K, Riese MJ, Gershan J, et al. STING agonist inflames the pancreatic cancer immune microenvironment and reduces tumor burden in mouse models. J Immunother Cancer 2019;7:115. [PubMed: 31036082]
44. Brägelmann J, Lorenz C, Borchmann S, Nishii K, Wegner J, Meder L, et al. MAPK-pathway inhibition mediates inflammatory reprogramming and sensitizes tumors to targeted activation of innate immunity sensor RIG-I. Nat Commun 2021;12:5505. [PubMed: 34535668]
45. Witkiewicz AK, McMillan EA, Balaji U, Baek G, Lin W-C, Mansour J, et al. Whole-exome sequencing of pancreatic cancer defines genetic diversity and therapeutic targets. Nat Commun 2015;6:6744. [PubMed: 25855536]
46. Kun E, Tsang YTM, Ng CW, Gershenson DM, Wong KK. MEK inhibitor resistance mechanisms and recent developments in combination trials. Cancer Treat Rev 2021;92:102137. [PubMed: 33340965]
47. Infante JR, Somer BG, Park JO, Li C-P, Scheulen ME, Kasubhai SM, et al. A randomised, double-blind, placebo-controlled trial of trametinib, an oral MEK inhibitor, in combination with gemcitabine for patients with untreated metastatic adenocarcinoma of the pancreas. Eur J Cancer 2014;50:2072–81. [PubMed: 24915778]
48. Post AEM, Smid M, Nagelkerke A, Martens JWM, Bussink J, Sweep FCGJ, et al. Interferon-stimulated genes are involved in cross-resistance to radiotherapy in tamoxifen-resistant breast cancer. Clin Cancer Res 2018;24:3397–408. [PubMed: 29661777]
49. Weichselbaum RR, Ishwaran H, Yoon T, Nuyten DSA, Baker SW, Khodarev N, et al. An interferon-related gene signature for DNA damage resistance is a predictive marker for chemotherapy and radiation for breast cancer. Proc Natl Acad Sci U S A 2008;105:18490–5. [PubMed: 19001271]
50. Benci JL, Johnson LR, Choa R, Xu Y, Qiu J, Zhou Z, et al. Opposing functions of interferon coordinate adaptive and innate immune responses to cancer immune checkpoint blockade. Cell 2019;178:933–48. [PubMed: 31398344]
51. Katlinskaya YV, Katlinski KV, Yu Q, Ortiz A, Beiting DP, Brice A, et al. Suppression of Type I interferon signaling overcomes oncogene-induced senescence and mediates melanoma development and progression. Cell Rep 2016;15:171–80. [PubMed: 27052162]
52. Katlinski KV, Gui J, Katlinskaya YV, Ortiz A, Chakraborty R, Bhattacharya S, et al. Inactivation of interferon receptor promotes the establishment of immune privileged tumor microenvironment. Cancer Cell 2017;31:194–207. [PubMed: 28196594]

Author Manuscript Author Manuscript Author Manuscript Author Manuscript

53. Padariya M, Sznarkowska A, Kote S, Gómez-Herranz M, Mikac S, Pilch M, et al. Functional interfaces, biological pathways, and regulations of interferon-related DNA damage resistance signature (IRDS) genes. Biomolecules 2021;11:622. [PubMed: 33922087]

54. Abt ER, Le TM, Dann AM, Capri JR, Poddar S, Lok V, et al. Reprogramming of nucleotide metabolism by interferon confers dependence on the replication stress response pathway in pancreatic cancer cells. Cell Rep 2022;38:110236. [PubMed: 35021095]

55. Punekar SR, Velcheti V, Neel BG, Wong KK. The current state of the art and future trends in RAS-targeted cancer therapies. Nat Rev Clin Oncol 2022;19:637–55. [PubMed: 36028717]

Author Manuscript Author Manuscript Author Manuscript Author Manuscript

Translational Relevance

A new generation of oncology drugs targeting stimulator of interferon genes (STING) has entered phase I clinical trials. STING agonists are primarily considered as immunostimulatory drugs, and combination strategies typically pair them with immune checkpoint inhibitors. This approach reflects the well-known functions of the STING signaling pathway in leukocytes and the presumed mechanism of their action in solid tumors, including pancreatic adenocarcinoma (PDAC). However, unlike other solid tumors, PDAC expresses robust tumor cell–intrinsic STING. Identifying drugs that work synergistically with STING agonists in PDAC should consider their direct activity on tumor cells, independent of tumor immunity. Herein, we provide mechanistic evidence that MEK inhibition uncovers the full potency of STING activation in PDAC through autocrine type I IFN signaling that directly kills tumor cells and increases survival in mouse models.

Author Manuscript Author Manuscript Author Manuscript Author Manuscript

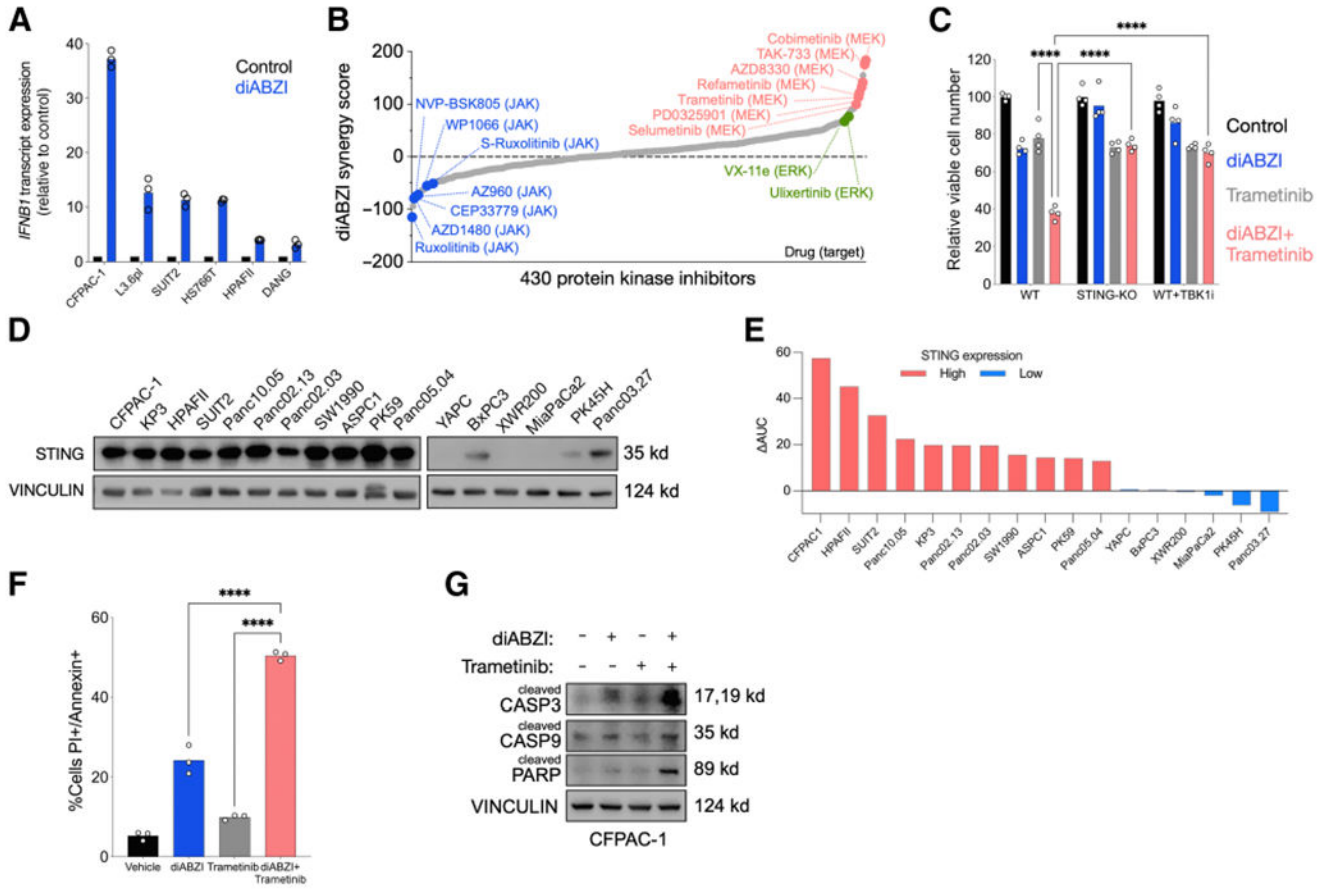

Figure 1.

STING agonist diABZI is synergistically cytotoxic with MEK inhibition in PDAC cell lines with high STING expression. **A,** Mean *IFNB1* gene expression in a panel of human PDAC cell lines ± 1 μmol/L diABZI exposure for 24 hours (bars represent means, three replicates shown). **B,** Synergy scores for 430 kinase inhibitors (7 nmol/L to 5 μmol/L each) and STING activation with 1 μmol/L diABZI in CFPAC-1 cells ($N = 2$ for each drug). Synergistic MEKi, ERK inhibitors, and antagonistic JAK inhibitors are indicated in red, green, and blue, respectively. **C,** The effect of diABZI and trametinib on expansion of CFPAC-1 cells (parental, *STING*-deficient, or parental with TBK1 inhibition) *in vitro* for 72 hours as measured by CellTiter-Glo (CTG; bars represent means, four replicates shown). **D,** Immunoblot analysis of baseline STING expression in a panel of human PDAC cell lines. **E,** The effect of 1 μmol/L diABZI on trametinib dose-response curves (by CTG) on a panel of human PDAC cell lines; *y*-axis represents the difference between area under the curve (ΔAUC) of diABZI + trametinib and trametinib only; larger positive values indicate stronger synergy. **F,** The percentage of dead CFPAC-1 cells (Annexin V+ PI+) by flow cytometry after culture with ± 1 μmol/L diABZI ± 200 nmol/L trametinib for 72 hours (bars represent means, three replicates shown; one-way ANOVA). **G,** Immunoblot analysis of apoptotic indicators in CFPAC-1 cells cultured ± 1 μmol/L diABZI ± 200 nmol/L trametinib for 24 hours. ***, $P < 0.001$; ****, $P < 0.0001$.

Author Manuscript Author Manuscript Author Manuscript Author Manuscript

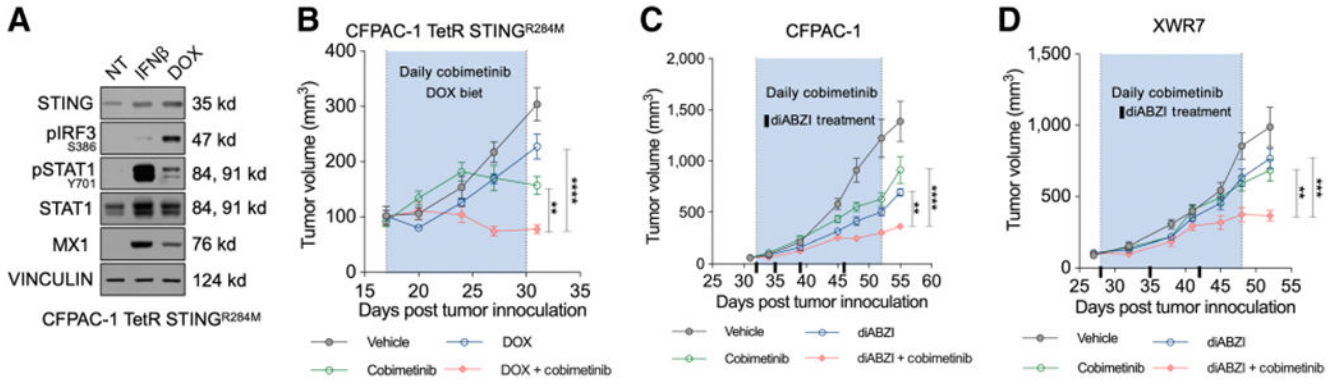

Figure 2.

STING activation synergizes with MEK inhibition to suppress xenografts of CFPAC-1 and a patient-derived tumor. **A,** Immunoblot analysis of CFPAC-1 TetR STING^{R284M} cells ± 100 U/mL IFNβ or 50 ng/mL DOX for 24 hours. **B,** Growth of CFPAC-1 TetR STING^{R284M} subcutaneous xenografts in mice ± DOX diet and/or ± 5 mg/kg cobimetinib daily for the range of days shaded blue. **C,** Growth of CFPAC-1 subcutaneous xenograft tumors in mice treated ± 1.5 mg/kg diABZI (for days indicated on the x-axis by black bars) and/or ± 5 mg/kg cobimetinib daily. **D,** Growth of xenografts of XWR7 patient-derived tumors treated ± 1.5 mg/kg diABZI (for days indicated on the *x*-axis by black bars) and/or ± 5 mg/kg cobimetinib daily. Tumor volumes for all experiments were measured by caliper (mean ± SEM; $N = 6–8$). **, $P < 0.01$; ***, $P < 0.001$).

Author Manuscript Author Manuscript Author Manuscript Author Manuscript

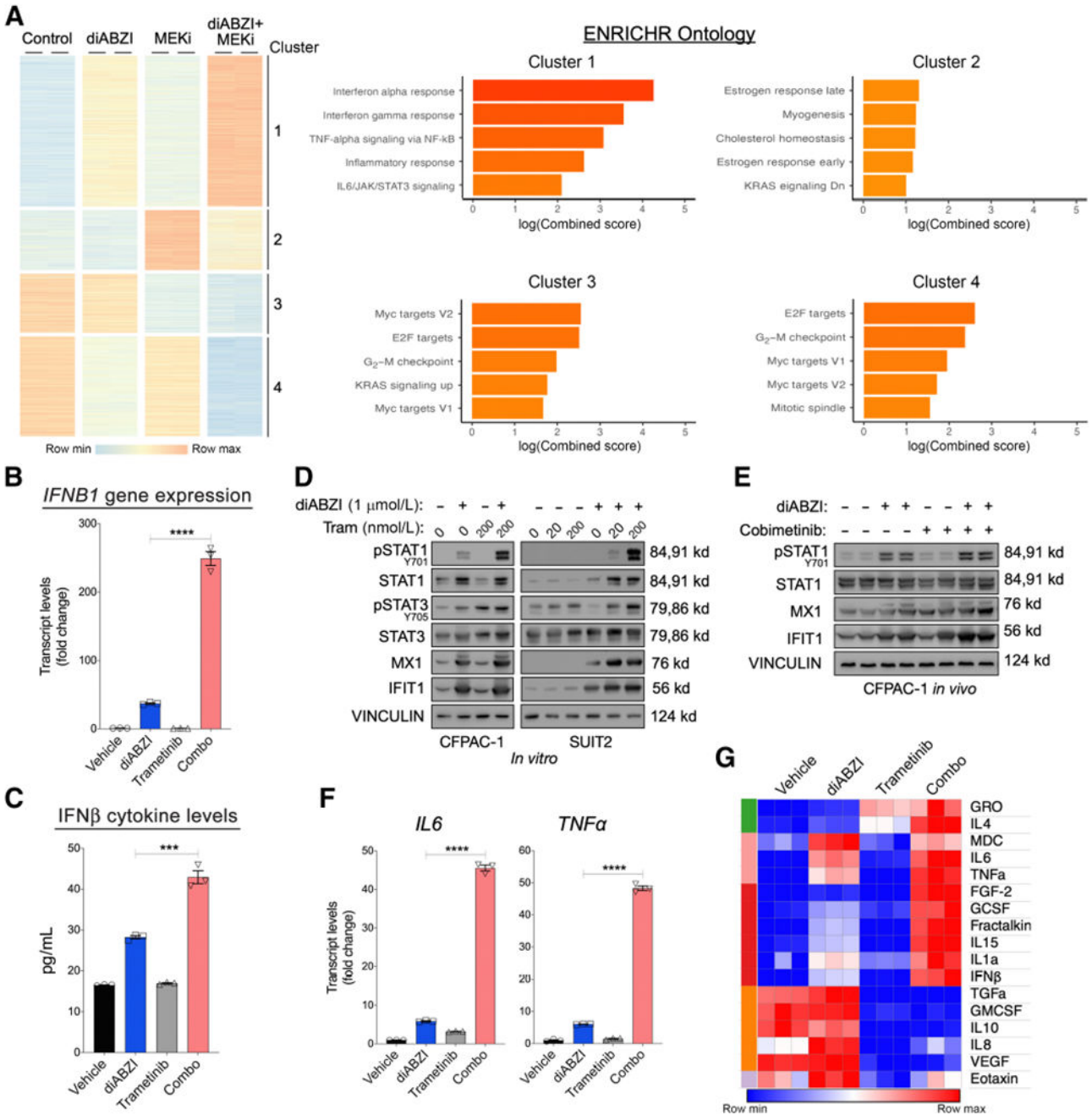

Figure 3.

MEK inhibition amplifies STING-mediated type I IFN and NFκB activity *in vitro* and *in vivo*. **A,** RNA-seq analysis of CFPAC-1 cells 24 hours after treatment ± 1 μmol/L diABZI ± 100 nmol/L trametinib using biological duplicates. The 11,260 genes with treatment-linked alterations in expression were clustered into four groups (heatmap, left). The top five gene expression pathways as determined by ENRICHR are given for each of the four clusters (right). **B,** RT-PCR analysis of *IFNB1* transcript levels in CFPAC-1 cells after 24 hours of culture ± 1 μmol/L diABZI ± 100 nmol/L trametinib (mean ± SEM; $N = 3$). **C,** ELISA

Author Manuscript Author Manuscript Author Manuscript Author Manuscript

detection of IFNβ in supernatants from 24 hours of culture of CFPAC-1 cells ± 1 μmol/L diABZI ± 100 nmol/L trametinib (mean ± SEM; $N = 3$). **D,** Immunoblot analysis of CFPAC-1 (left) and SUIT2 (right) cells after 24 hours of culture ± 1μmol/L diABZI ± 100 nmol/L trametinib. **E,** Immunoblot analysis of subcutaneous tumors of CFPAC-1 cells in NSG mice, 24 hours after single dose of ± 1.5 mg/kg diABZI i.v ± 5 mg/kg cobimetinib orally ($N = 2$). **F,** RT-PCR analysis of *IL6* (left) and *TNF* (right) gene expression in CFPAC-1 cells after 24 hours of culture ± 1 μmol/L diABZI ± 100 nmol/L trametinib for 24 hours (mean ± SEM; $N = 3$). **G,** Heatmap representing relative expression of select drug-responsive cytokines from a human 38-plex chemokine/cytokine luminex assay of cultured media collected 24 hours after culture of CFPAC-1 cells ± 1 μmol/L diABZI ± 100 nmol/L trametinib. ***, $P < 0.001$; ****, $P < 0.0001$.

Author Manuscript Author Manuscript Author Manuscript Author Manuscript

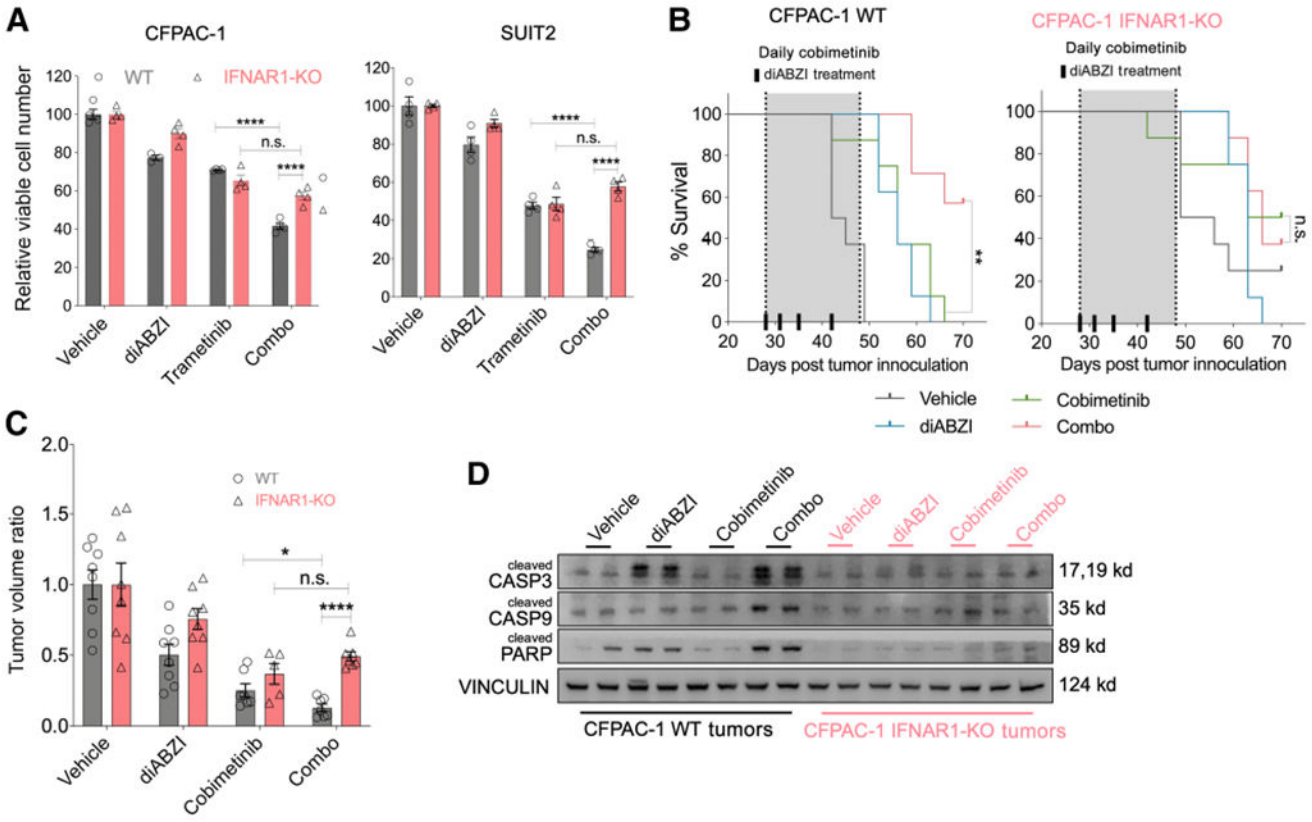

Figure 4.

Type I IFN signaling is essential for the synergy between STING agonist and MEKi *in vitro* and *in vivo*. **A,** Proliferation of WT and IFNAR1-KO CFPAC-1 (left chart) and SUIT2 (right chart) cells in response to ±1 μmol/L diABZI ± 100 nmol/L trametinib for 72 hours as measured by the CTG assay (mean ± SEM; $N = 4$). **B,** Percentage of mice surviving with CFPAC-1 parental (left) or IFNAR1-KO (right) xenografts ≤ 500 mm^3 after treatment ± 1.5 mg/kg diABZI (for days indicated on the *x*-axis by black bars) and/or ± 5 mg/kg cobimetinib daily. **C,** Vehicle cohort-normalized tumor volumes from cross-sectional analysis of xenografts 52 days after implantation with the treatment regimens described for **B** (mean ± SEM; $N = 8$). **D,** Immunoblot analysis of CFPAC-1 (WT and IFNAR1-KO) xenografts 24 hours after treatment ± 1.5 mg/kg diABZI i.v ± 5 mg/kg cobimetinib ($N = 2$). *, $P < 0.05$; **, $P < 0.01$; ****, $P < 0.0001$. WT, wild-type.

Author Manuscript Author Manuscript Author Manuscript Author Manuscript

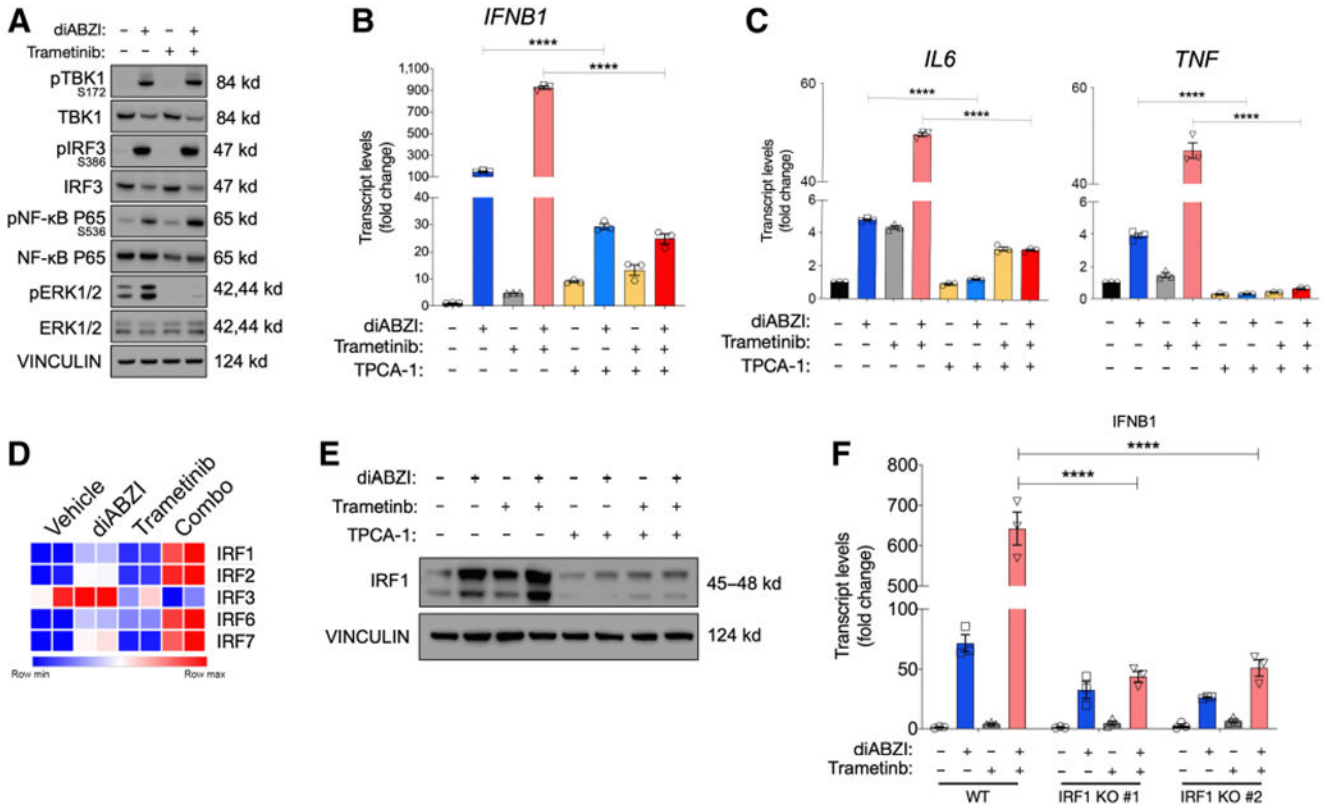

Figure 5.

NFκB mediates the synergistic effects of STING activation and MEK inhibition through IRF1. **A,** Immunoblot analysis of CFPAC-1 cells cultured ± 1 μmol/L diABZI ± 100 μmol/L trametinib for 24 hours. **B,** RT-PCR analysis of *IFNB1* expression in CFPAC-1 cells cultured ±1 μmol/L diABZI ± 100 nmol/L trametinib ± 10 μmol/L TPCA-1 (IKK-2 inhibitor) for 24 hours (mean ± SEM; $N = 3$). **C,** RT-PCR analysis of *IL6* (left) and *TNFA* (right) gene expression in CFPAC-1 cells cultured ± 1 μmol/L diABZI ± 100 nmol/L trametinib ± 10 μmol/L TPCA-1 (IKK-2 inhibitor) for 24 hours (mean ± SEM; $N = 3$). **D,** Relative gene expression of IRF family members in CFPAC-1 cells cultured ± 1 μmol/L diABZI ± 100 nmol/L trametinib. **E,** Expression of IRF1 in CFPAC-1 cells after 24 hours of culture ± 1 μmol/L diABZI ± 100 nmol/L trametinib ± 10 μmol/L TPCA-1. **F,** RT-PCR analysis of *IFNB1* gene expression in parental or IRF1-deficient CFPAC-1 cells after 24 hours of culture ± 1 μmol/L diABZI ± 100 nmol/L trametinib.

Author Manuscript Author Manuscript Author Manuscript Author Manuscript

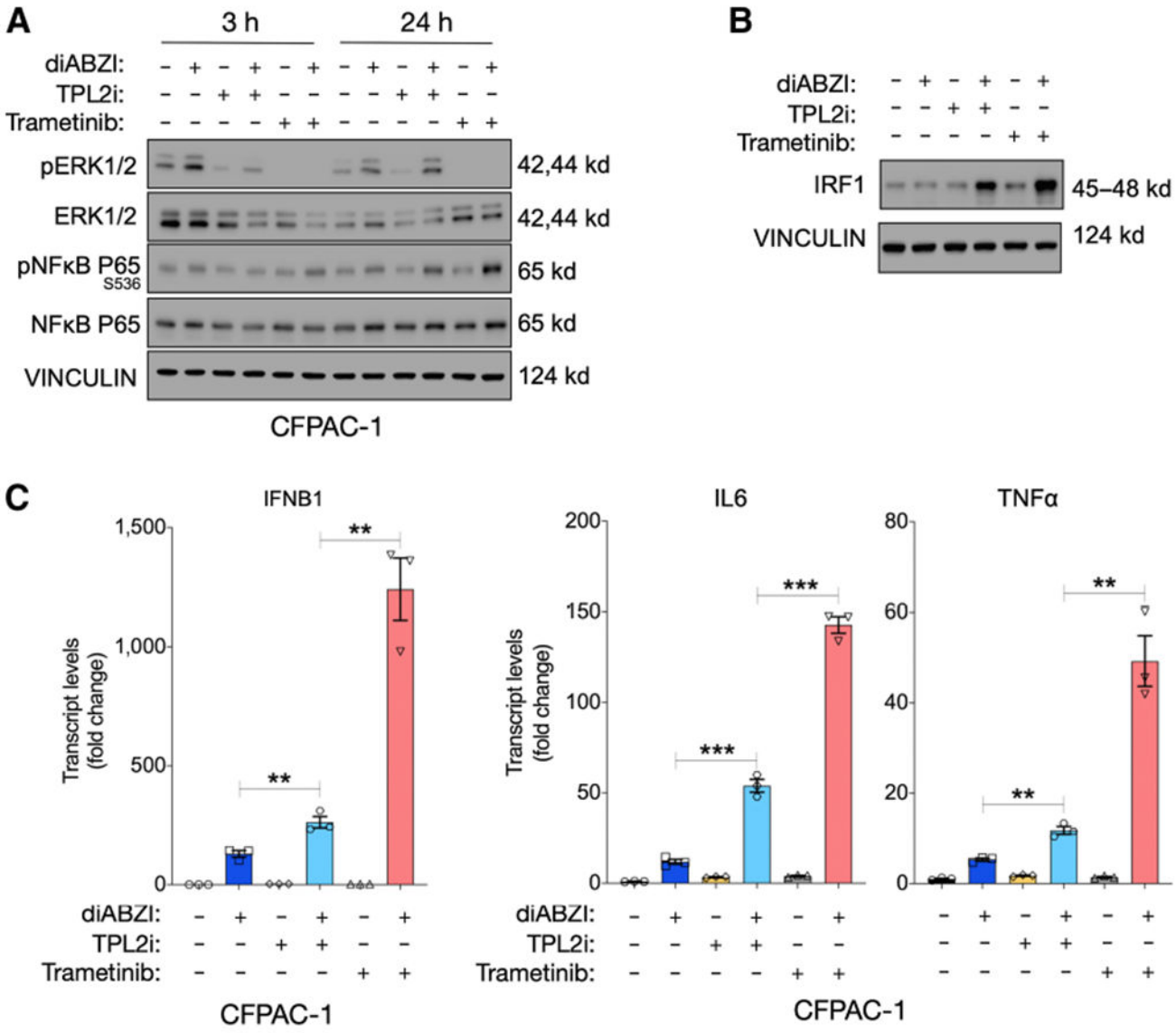

Figure 6.

Activation of MEK by TPL2 inhibits activation of NFκB by STING. **A,** Immunoblot analysis of CFPAC-1 cells cultured for 3 or 24 hours ± 1 μmol/L diABZI ± 100 nmol/L trametinib ± 10 μmol/L TPL2i. **B,** Immunoblot analysis of IRF1 expression in CFPAC-1 cells cultured for 24 hours ± 1 μmol/L diABZI ± 100 nmol/L trametinib ± 10 μmol/L TPL2i. **C,** RT-PCR analysis of *IFNB1, IL6*, and *TNF* expression in CFPAC-1 cells treated ± 1 μmol/L diABZI ± 100 nmol/L trametinib ± 10 μmol/L TPL2i for 24 hours (mean ± SEM; *N* = 3).

Author Manuscript Author Manuscript Author Manuscript Author Manuscript

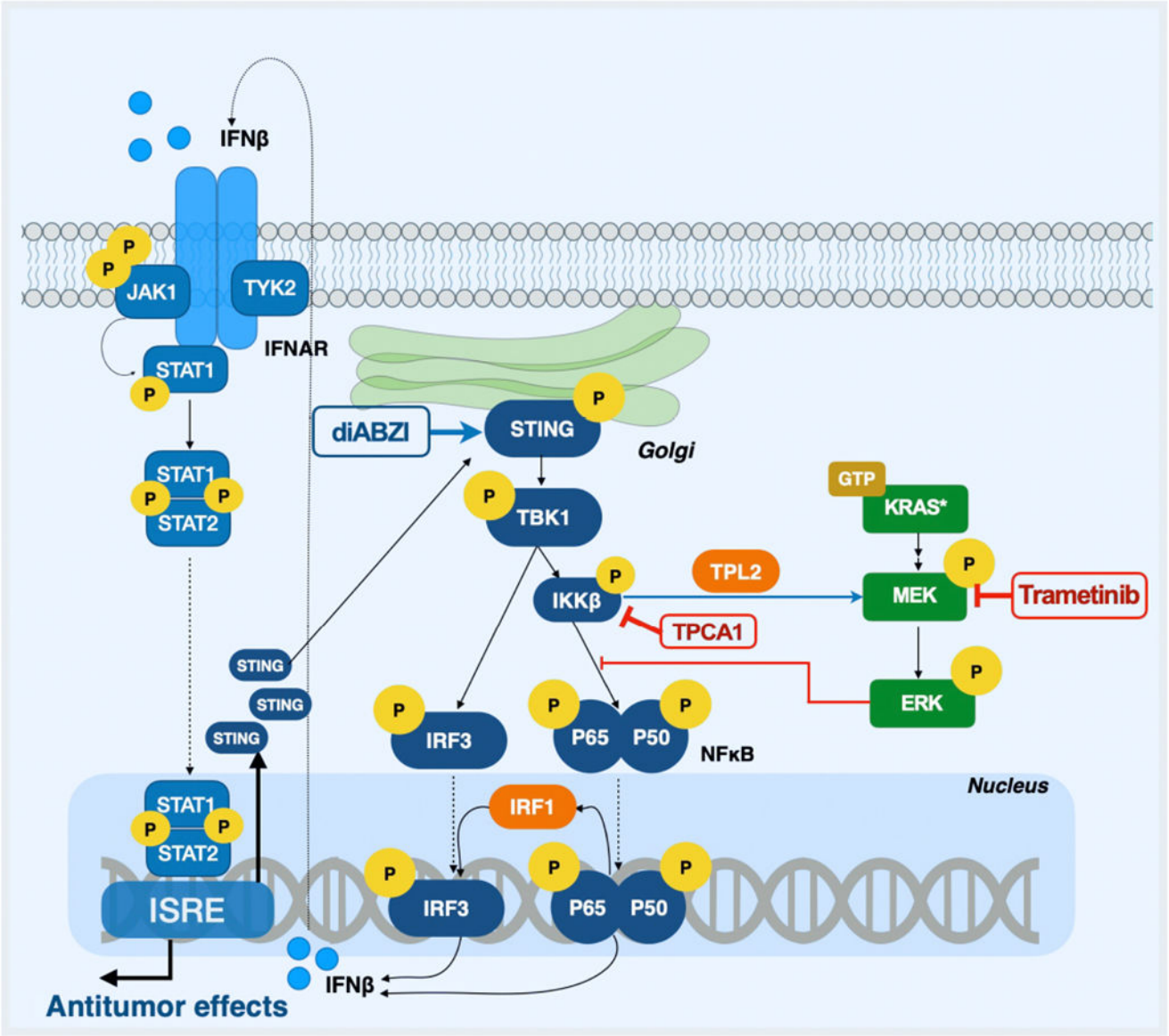

Figure 7.

Relevant pathways linking STING, MEK, and IFN activity. Activation of the STING pathway (dark blue) through TBK1 and IRF3 by diABZI drives a kinase activation cascade leading to IRF3-driven transcription of IFNβ. In turn, IFNβ can trigger cell-intrinsic signaling (light blue) through the IFN receptor mediated by JAK/STAT signaling and leading to transcription activation from interferon-sensitive response elements (ISRE) and expression of ISG. STING itself is an ISG promoting feed-forward IFN effects. In parallel to IFN stimulation, STING activation also activates IKKβ derepression of NFκB (p65/p50) and resultant expression of IRF1 that further promotes IFNβ expression. MEK/ERK signaling (green) represses NFκB activation. Inhibition of MEK/ERK signaling by trametinib,

TPCA1, or inhibition of TPL2 allows robust NFκB activation, furthering IFN-mediated intrinsic cytotoxicity.

Author Manuscript Author Manuscript Author Manuscript Author Manuscript

Author Manuscript Author Manuscript Author Manuscript Author Manuscript

Key Resources

Reagent	Source	Identifier
DMEM	Corning	10-107-CV
RPMI 1640	Corning	10-040-CV
Fetal bovine serum	Omega Scientific	FB-11
Dialyzed fetal bovine serum	Omega Scientific	FB-03
Lipofectamine 3000	ThermoFisher Scientific	L3000001
OptiMEM	ThermoFisher Scientific	31985-062
Polyethyleneimine	Polysciences	23966-1
Human IFNβ	PBL Assay Science	11415-1
Human Recombinant IL-6	PeproTech	200-06
diABZI	Selleckchem	S8796
Trametinib	Selleckchem	S2673
Cobimetinib	Selleckchem	S8041
SCH772984	Selleckchem	S7101
SC144	Selleckchem	S7124
TPL2 inhibitor	Cayman	19710
Tocilizumab	Selleckchem	A2012
TPCA1	Selleckchem	S2824
Z-VAD-FMK	InvivoGen	tlrl-vad
Doxycycline	Clontech	631311
BCA assay	ThermoFisher Scientific	23225
RIPA protein lysis buffer	Boston BioProducts	BP-115
Laemmli loading dye	Boston BioProducts	BP-110R
4-12% bis-tris gels	ThermoFisher Scientific	NP0336
Nitrocellulose membrane	ThermoFisher Scientific	88018
Nonfat dry milk	ThermoFisher Scientific	M-0841
Tris-buffered saline	ThermoFisher Scientific	50-751-7046
Tween-20	Sigma-Aldrich	P9416
Bovine Serum Albumin	Fisher Scientific	9048-46-8
Halt protease inhibitor cocktail	ThermoFisher Scientific	PI78430
Halt phosphatase inhibitor cocktail	ThermoFisher Scientific	PI78428
Immobilon Western HRP Substrate - Forte	Millipore	WBLUF0500
NucleoSpin RNA	Takara	740955.250
MultiScribe Reverse Transcriptase	ThermoFisher Scientific	4311235
2x qPCR Universal Green MasterMix	Lamda Biotech	qMX-Green
Hard tissue homogenizing vials	Omni International	19-628
Halt protease inhibitor cocktail	ThermoFisher Scientific	PI78430
Halt phosphatase inhibitor cocktail	ThermoFisher Scientific	PI78428
White 2D Opaque 384-well Plate	Greiner BioOne CellStar	82051-278
Doxycycline supplemented rodent diet	Envigo	TD.120769

Author Manuscript Author Manuscript Author Manuscript Author Manuscript

Reagent	Source	Identifier
Control rodent diet	Envigo	TD.00588
PEG-400	Millipore Sigma	PX1286B-2
Critical Commercial Assay	**Source**	**Identifier**
VeriKline Human IFN Beta ELISA	PBL Assay Science	41410-1
2D CellTiterGlo Cell Viability Assay	Promega	G7572
RealTime-Glo MT Cell Viability Assay	Promega	G9711
Annexin-V FITC Apoptosis Kit	BioVision	K101-25
MycoPlasma Detection Kit	Sigma-Aldrich	MP0025
Antibodies	**Source**	**Identifier**
TOTAL STAT1	Cell Signaling Technology	14994
PHOSPHO STAT1 Y701	Cell Signaling Technology	9167
MX1	Cell Signaling Technology	37849
VINCULIN	Cell Signaling Technology	13901
TYMP	Cell Signaling Technology	4307
TOTAL STAT3	Cell Signaling Technology	9139
PHOSPHO STAT3 Y705	Cell Signaling Technology	9145
PHOSPHO STING S366	Cell Signaling Technology	50907
STING (TMEM173)	Cell Signaling Technology	13647
TBK1	Cell Signaling Technology	3013
PHOSPHO TBK1 S172	Cell Signaling Technology	5483
PHOSPHO IRF3 S386	Abcam	76493
IRF3	Cell Signaling Technology	4302
NFKB P65	Cell Signaling Technology	8242
PHOSPHO NFKB P65 S536	Cell Signaling Technology	3033
P44/42 MAPK (ERK1/2)	Cell Signaling Technology	4695
PHOSPHO P44/42 MAPK (pERK1/2)	Cell Signaling Technology	4370
CLEAVED CASPASE 3	Cell Signaling Technology	9662
CLEAVED CASPASE 9	Cell Signaling Technology	20750
CLEAVED PARP	Cell Signaling Technology	5625
BIM	Cell Signaling Technology	2933
PHOSPHO H2AX S139	Cell Signaling Technology	9718
IFNAR1	Santa Cruz Biotechnology	7391
IFIT1	Cell Signaling Technology	14769
IRF1		
ANTI-RABBIT IgG, HRP-LINKED	Cell Signaling Technology	7074
ANTI-MOUSE IgG, HRP-LINKED	Cell Signaling Technology	7076
RT-PCR Primer	**Forward**	**Reverse**
human IFNβ1	CAGCAATTTTCAGTGTCAGAAGC	TCATCCTGTCCTTGAGGCAGT
human IL6	AATTCGGTACATCCTCGACGG	GGTTGTTTTCTGCCAGTGCC

Author Manuscript

Author Manuscript

Author Manuscript

Author Manuscript

Reagent	Source	Identifier
human TNFA	CCCAGGCAGTCAGATCATCTTC	TCTCTCAGCTCCACGCCATT
human ACTIN	CATGTACGTTGCTATCCAGGC	CTCCTTAATGTCACGCACGAT
gRNA Sequence	**#1**	**#2**
IFNAR1 KO	GCACTAGGGTCGTCGCGCCC	GCTCGTCGCCGTGGCGCCAT
IL6R KO	CACCCATCCCTGACGACAA	TGCATCCGCCGTACTCTTTG
IRF1 KO	TCTAGGCCGATACAAAGCAG	CACCTCCTCGATATCTGGCA
STING KO	GCATGCTTAGGGACTTATAG	GTCCAAGTTCGTGCGAGGCT
Software	**Source**	**Identifier**
Prism 7	GraphPad Software	N/A
Flowjo 7.6	TreeStar	N/A
Instrument	**Manufacturer**	**Assay**
Attune NxT	ThermoFisher	Flow Cytometry
Microplate reader	BioTek	Luminesence Cell Viabilioty Assays
BeadRuptor Elite	OMNI International	Tissue Homogenization
Odyssey Fc Imaging System	LI-COR	Western Blot Reading
QunatStudio3 RT-PCR System	Applied Biosystems	qRT-PCR